



Original article

Potential cytotoxicity of silver nanoparticles: Stimulation of autophagy and mitochondrial dysfunction in cardiac cells

Azmat Ali Khan*, Amer M. Alanazi, Nawaf Alsaif, Mohammad Al-anazi, Ahmed Y.A. Sayed, Mashooq Ahmad Bhat

Pharmaceutical Biotechnology Laboratory, Department of Pharmaceutical Chemistry, College of Pharmacy, King Saud University, Riyadh 11451, Saudi Arabia

ARTICLE INFO

Article history:

Received 2 February 2021

Revised 6 March 2021

Accepted 7 March 2021

Available online 17 March 2021

Keywords:

Nanoparticles

Autophagy

ROS

Cardiomyocytes

Mitochondrial dysfunction

ABSTRACT

In the present study, we elucidated the potential cytotoxicity of AgNPs in H9c2 rat cardiomyoblasts and assessed the underlying toxicological manifestations responsible for their toxicity thereof. The results indicated that the exposure of AgNPs to H9c2 cardiac cells decreased cell viability in a dose-dependent manner and caused cell cycle arrest followed by induction of apoptosis. The AgNPs treated cardiac cells showed a generation of reactive oxygen species (ROS) and mitochondrial dysfunction where mitochondrial ATP was reduced and the expression of AMPK1 α increased. AgNPs also induced ROS-mediated autophagy in H9c2 cells. There was a significant time-dependent increase in intracellular levels of Atg5, Beclin1, and LC3BII after exposure to AgNPs, signifying the autophagic response in H9c2 cells. More importantly, the addition of N-acetyl-L-cysteine (NAC) inhibited autophagy and significantly reduced the cytotoxicity of AgNPs in H9c2 cells. The study highlights the prospective toxicity of AgNPs on cardiac cells, collectively signifying a potential health risk.

© 2021 Published by Elsevier B.V. on behalf of King Saud University. This is an open access article under the CC BY-NC-ND license (<http://creativecommons.org/licenses/by-nc-nd/4.0/>).

1. Introduction

The burgeoning field of nanotechnology offers many potential benefits to the allied field of biomedical sciences. With advancements in the field of nanotechnology, the application of nanoparticles (NPs) has increased tremendously over the years. The use of drug delivery systems has smartly substituted a conventional drug dosage form and has emerged as a promising tool in nanomedicine (Nikalje, 2015). The innovative approach of nanosystems has shown a profound effect on diagnosis, imaging, sensing, treatment, and control; thereby improving human health and disease (Emerich and Thanos, 2003). Over the years, a large variety of NPs like liposomes, dendrimers, quantum dots, metallic NPs, nanotubes, etc. has been investigated for their application in nanomedicine, therapy, and diagnostics (Abhilash, 2010). Since past

decades, NPs with exceptional catalytic, magnetic, electrical, and optical properties are being engineered and further modified to enhance their use as diagnostic and therapeutic agents (Emeje et al., 2012; Khan et al., 2018; Srinivasan et al., 2015). They have a wide range of emerging applications in cell and molecular biology, cancer diagnosis and therapy, photodynamic therapy, diagnostic imaging etc (Allison et al., 2008; Hu et al., 2010; Wang and Wang, 2014).

Metallic NPs have a wide spectrum of aspects in health and pharmaceutical applications. These materials have received much recognition because of their number of useful properties and multi-potential features that are required for commercial production. They have unlocked many new pathways and today, scientists are showing interest in their applications in the field of biomedicine (Edmundson et al., 2014). Parallel to these aspects, concerns regarding the risk of metallic NPs to human health and surrounding has also been increased (Service, 2004). Various research fraternities have highlighted the untoward effects of different NPs including carbon nanotubes (CNTs), titanium oxide (TiO₂) NPs, cadmium (Cd) NPs, etc. (Carro et al., 2019; Huerta-Garcia et al., 2018; Joviano-Santos et al., 2014; Kavosi et al., 2018; Ladhar et al., 2014; Pujalte et al., 2011; Rana et al., 2018). Studies have revealed differential cardiovascular toxicities of single- and multi-wall CNTs (Joviano-Santos et al., 2014; Kavosi et al., 2018). Lopez-Marure

* Corresponding author.

E-mail address: azkhan@ksu.edu.sa (A.A. Khan).

Peer review under responsibility of King Saud University.



Production and hosting by Elsevier

and group have demonstrated the toxicity of TiO₂ in cardiac cells (Huerta-Garcia et al., 2018). Furthermore, ultrafine NPs are shown to translocate through systemic circulation and have been associated with cardiovascular morbidity and mortality (Brown et al., 2001; Dailey et al., 2006; Hamoir et al., 2003; Nemmar et al., 2001; Oberdorster, 2001).

Among various types of metallic NPs; silver NPs (AgNPs) is one of the most attractive and profoundly used metallic NPs with applications in diagnostics, photography, biosensors, catalysis, etc. (Hussain et al., 2011; Sun and Seff, 2011). Silver since ancient times has been known for its capability to combat infections and has been used in medical treatments. It is also known for its antibacterial, antiseptic, anticancer, and anti-inflammatory properties (Chernousova and Epple, 2013; Sintubin et al., 2011). To exploit the full potential of silver in a varied range of applications, innovative methods have been utilized for the synthesis of AgNPs. Chemical and physical methods of synthesis are the most conventional methods that are used but due to the requirement of special equipment and toxic chemicals they are very expensive and hazardous (Gurunathan et al., 2015; Li et al., 2012; Zhang et al., 2016). Simple and environment-friendly biological methods have attracted considerable attention as they are cost-effective and have shown high sustainability and stability. Biological sources like bacteria, fungi, yeasts, plants, small biomolecules like amino acids and vitamins have remarkably become a simple and alternative route of synthesis (Abdeen et al., 2014; Karthik et al., 2014; Ratan et al., 2020; Shankar and Rhim, 2015; Sunkar and Nachiyar, 2012).

In the realms of NPs with biomedical potentialities; AgNPs are one of the highest profitable products; widely used in commercialized products like cosmetics, nanomedical devices, clothing, sprays, household, and food products. Owing to their nano sizes they can reach tissues and organs and could easily cause adverse effects on humans and other organisms. Moreover, AgNPs are directly related to an immune response. They are known to regulate both cellular and humoral immune responses. Hence, due to the increase in manufacturing and utilization; AgNPs are inevitably posing a high potential risk to human health and surrounding (Gonzalez et al., 2016). Direct human contact of AgNPs would likely be nearly unavoidable in the coming future. Exposure to AgNPs has shown increased oxidative stress, genotoxicity, and apoptosis in *in vitro* studies (Lee et al., 2014; Reetta et al., 2019). Studies have demonstrated direct accumulation of AgNPs in different organs (Quadros & Marr, 2010); and it has also been shown that AgNPs could translocate through the blood to various organs of the body (Anwar et al., 2015; Sun et al., 2016). AgNPs instillation has been shown to aggravate cardiac ischemia/ reperfusion injury (Holland et al., 2016). Studies done on animals of AgNPs exposure have shown enhanced production of anions and harmful effects in cardiac tissues (Gonzalez et al., 2016; Lin et al., 2017; Rahman et al., 2009; Xu et al., 2018). It is relatable that the interaction of AgNPs with the cardiovascular system is relatively high. It is important to note that major toxicity concern of AgNPs in the cardiovascular system is that it limits the translation for cardiac tissue repair. This warrants further evaluation of the interaction of AgNPs with the cardiovascular system.

Considering these aspects, in this research endeavor, we evaluated the direct effects of AgNPs on H9c2 cardiac cells. Essentially, H9c2 cardiomyoblasts show hypertrophic responses that are similar to those of primary rat neonatal cardiomyocytes *in vitro* (Watkins et al., 2011). To the best of our knowledge, there is no study, wherein the effects of AgNPs on H9c2 cardiomyoblasts have been investigated. The potential cytotoxicity of AgNPs on cardiac cells was assessed and their toxic manifestations were investigated thereof. Interestingly, this is a pioneer report providing an insight into the putative toxic manifestations of AgNPs on H9c2 cardiac cells.

2. Materials and methods

2.1. Chemicals and reagents

AgNO₃ (CAS No. 7761-88-8), NaBH₄ (CAS No.16940-66-2), N-acetyl-L-cysteine (NAC), 2, 7-dichlorofluorescein diacetate (CAS No. 4091-99-0), 5-bromo-2-deoxyuridine (BrdU; CAS No. 59-14-3) and Dulbecco's Minimal Essential Medium (DMEM; CAS No. D5030-10L) were procured from Sigma Aldrich, USA. cDNA Synthesis kit was purchased from Fermentas, USA. Alexa 488-labelled antibodies were obtained from Molecular Probes. The Cell Titer-Glo Luminescent cell viability assay kit was procured from Promega Corp. (Madison, WI, USA). Anti-Atg5, Anti-Beclin1, anti-LC3B, Anti-pAMPK1 α , Anti-GAPDH, Anti- β -actin, and rabbit anti-mouse horseradish peroxidase (HRP)-labeled secondary antibodies were procured from Cell Signaling Technology. Enhanced chemiluminescence (ECL) system kit, sterile filters (0.22 μ m), and polyvinylidene difluoride (PVDF) membranes were procured from Millipore (MA, USA). DNA fragmentation ELISA kit was procured from Roche Diagnostics, Mannheim, Germany. All the chemicals used were of the highest purity grade. All the plastic wares used in the study for cell culture were procured from Thermo Fisher Scientific, USA.

2.2. H9c2 cardiomyoblast cell culture

H9c2 cardiomyoblasts were obtained from the ATCC (CRL-1446), Manassas, VA, USA. H9c2 cardiomyoblasts were cultured in standard DMEM culture medium supplemented with 10% FBS, 2 mM glutamine, 100 U/mL penicillin, 100 mg/mL streptomycin, and 1 mM pyruvate under standard culture conditions of 5% CO₂ with 95% humidity at 37 °C. Cells were screened periodically for mycoplasma contamination.

2.3. Synthesis of AgNPs

AgNPs were synthesized following previously published protocol as standardized in the lab (Irvani et al., 2014; Kumar et al., 2019). Freshly prepared aqueous solution of NaBH₄ (1.0 mM) was prepared and stirred on a magnetic stirrer at a speed of 800 rpm and the solution was heated to 60 °C. Thereafter, to this solution, ice-cold AgNO₃ (1.0 mM) was added in a drop-wise manner. The resulting solution was stirred and heated unless a change of color was observed; which is indicative of the formation of AgNPs. Finally, the NPs suspension was cooled at room temperature (RT), centrifuged, washed thrice with PBS, and finally stored at 4 °C for future experiments.

2.4. Characterization of the as-synthesized AgNPs

The as-synthesized AgNPs were examined through UV/VIS Spectro-fluorometer (Jasco, FP-8200). The absorption spectra were measured between 300 and 800 nm. For Transmission Electron Microscopy (TEM), a drop of AgNPs was mounted over gold-coated negative grid of transmission electron microscope (Model HT 7700, Hitachi High Technologies, America Inc.) followed by evaporation of the solvent. The analysis was performed at an accelerating voltage of 200 kV for their shape and morphology (Khan et al., 2017). Zeta-potential was measured according to the Smoluchowski equation. AgNPs were dispersed in an aqueous solution and the measurements were performed in triplicates on undiluted samples at 25 °C by Zeta Nano ZS (Malvern Instruments Ltd., Worcestershire, UK) (Khan et al., 2019).

2.5. MTT test

The effect of AgNPs on the viability of H9c2 cardiomyoblasts was examined using a standard MTT reduction assay (Khan et al., 2011). Briefly, cells (1×10^6 /well) were seeded in 96-well culture plates and grown in DMEM for 24 hr. The cells were treated with increasing concentration of AgNPs from 0 to 10 μ g/ml and incubated for 48 hr. Thereafter the medium was substituted with fresh medium and MTT reagent at a volume of 1:10 was added. After 4 hr, the reaction was stopped by adding DMSO and absorbance was taken. Half maximal inhibitory concentration (IC_{50}) was calculated and that dose was used in all the experiments.

2.6. Cellular DNA fragmentation ELISA

DNA fragmentation profile was examined through cellular DNA fragmentation ELISA kit (Roche Diagnostics, Mannheim, Germany) as delineated by the manufacturer. In brief, cells were labeled with 5-Bromo-2-deoxyuridine (BrdU) and then treated with AgNPs for a stipulated time intervals. Following treatment with AgNPs for 24 and 48 hr, the cells were harvested, lysed, and thereafter, labeled DNA was analyzed using an ELISA microtiter plate reader at 260 nm. Relative DNA fragmentation was calculated as a ratio of the absorbance of AgNPs exposed cells to control cells.

2.7. Cell cycle analysis

Cell cycle phase distribution in AgNPs treated cells were analyzed using a flow cytometer. Briefly, the cells were seeded in 6-well culture plates and after 24 hr were treated with AgNPs. Following desired treatment for 24 and 48 hr, the cells were harvested, washed, and fixed. After centrifugation cell suspension was incubated with RNase A for 60 min and then was incubated with propidium iodide (PI) for 30 min at RT. Data analysis was done using Cell Quest Pro software.

2.8. Immunofluorescence assay

For immunofluorescence assay, the previously published protocol of Fageria et al. (2017) was followed as standardized in our lab. Basically, cells were cultured in 6 cm culture plates, treated with AgNPs for a stipulated time interval. After these, cells were washed with PBS and fixed with 4% paraformaldehyde solution. The cells were made permeable with 0.1% Triton X-100 solution. Finally, after usual washing steps, the cells were blocked with 2% FCS and thereafter incubated with anti-LC3BII antibodies (1:50). After washing again, the cells were further incubated with Alexa 488-labeled secondary antibodies (1:100). Finally, the images were acquired through fluorescence microscopy (EVOS, Life Technologies, USA) and were processed using Adobe 7.0 (CA, USA).

2.9. DCFH-DA assay

To detect ROS generation, 2, 7-dichlorofluorescein diacetate (DCFH-DA) assay was employed. Basically, cells (1×10^6 /well) were seeded in 6-well culture plates. Following overnight culture, the cells were treated with AgNPs for 24 and 48 hr time interval. After these, the cells were harvested and re-suspended in PBS. Following this, the cells were incubated with DCFH-DA reagent for 30 min at RT. The samples were then analyzed with a flow cytometer (MACSQuant, Germany) following standard flow procedures. For fluorescence microscopic analysis, the cells were analysed under fluorescence microscope.

2.10. MitoSOX analysis

For mitosox analysis, cells were seeded in confocal plates and treated with AgNPs for 24 and 48 hr, separately. Following treatment with AgNPs for a stipulated time interval, the cells were washed with $1 \times$ PBS and incubated with MitoSOX with a final concentration of 5 μ M for 30 min. The cells were then analyzed with a confocal laser scanning microscope (LSM Pascal, Zeiss, Germany). Images were captured using 20X objective with excitation wavelength 514 nm (Mukhopadhyay et al., 2007).

2.11. Measurement of adenosine-5'-triphosphate (ATP) production

The ATP concentration was determined with Cell Titer-Glo Luminescent cell viability assay procured from Promega Corp. (Madison, WI, USA) following the company's recommended protocol. In brief, following treatment with AgNPs for a stipulated time interval, the cells were incubated with Cell Titer-Glo Reagent (Promega, USA) for 10 min to induce luminescent signals. Thereafter, the signals were acquired with a luminometer (Berthold, USA) (Iovine et al., 2012).

2.12. Western blot analysis

For Western blotting, cells from the control and AgNPs treated group was lysed in RIPA lysis buffer and the cell lysates were collected and quantified by NanoDrop 2000 (ThermoFisher Scientific) assay and stored at -20°C for subsequent studies. Basically, the cell lysates were resolved through 12%–15% SDS-PAGE and blotted to PVDF membranes (Millipore, MA, USA). The membranes were blocked with a blocking solution containing 5% milk in Tris-buffered saline Tween-20 (TBST) for 1 hr at RT and then washed with TBS-T thrice. The membranes were incubated with primary antibodies (1:1000) against Atg5, Beclin1, LC3B, pAMPK1 α , GAPDH, β -actin at 4°C for overnight. Concomitantly, after washing, the blots were incubated with horseradish peroxidase (HRP)-labeled secondary antibodies for 1 hr. Finally, the signals were acquired with enhanced chemiluminescence (ECL) system (Millipore, MA, USA) with LAS 3000 imaging system (Fujifilm, Tokyo, Japan).

2.13. N-acetyl-L-cysteine (NAC) inhibitor studies

For inhibitor study employing N-acetyl-L-cysteine (NAC), the H9c2 cells were pre-treated with 10 mM NAC for 2 hr and then were treated with AgNPs for 48 hr time interval. The treated NAC was analyzed through the following studies.

RNA isolation, cDNA synthesis and RT-PCR: The relative abundance of Beclin-1 and LC3BII were determined through RT-PCR following standard methods. Briefly, RNA from control and AgNPs treated H9c2 cells were extracted by employing Trizol reagent. The RNA was reverse-transcribed employing Revert Aid First Strand cDNA Synthesis kit following procedures delineated by the manufacturer. The relative abundance of Beclin-1 and LC3BII were assessed through RT-PCR employing SYBR green master mix. The primer sequences employed are given below (Jiang et al., 2012). The RT-PCR data was analyzed through the $2^{-\Delta\Delta Ct}$ method and the expression of target genes normalized to GAPDH expression was then represented in the form of a graph.

Primer

Beclin-1: Fwd-5'GGCTGAGAGACTGGATCAGG'3

Rev-5'CTGCGTCTGGCATAACG'3

LC3BII: Fwd-5'GAGAAGCAGCTTCTGTCTGG'3

Rev-5'GTGT CCGTTCACCAACAGGAAG'3

GAPDH: Fwd-5' GGACTGACCTGCCGTCTAG'3

Rev-5'TAGCCCAGG ATGCCCTTGAG'3

Further, the DNA fragmentation profile was examined through cellular DNA fragmentation ELISA kit (Roche Diagnostics, Mannheim, Germany) as outlined by the manufacturer and as described above. For DNA ladder assay, following treatment with AgNPs for a stipulated time interval, the cells were harvested; genomic DNA was extracted and finally analyzed through agarose gel electrophoresis.

2.14. Statistical analysis

Data are shown as mean \pm SE with at least three independent experiments. The data were statistically analyzed with one-way ANOVA followed by Tukey's test of significance using GraphPad Prism software. The statistical analysis was done using Sigma-Plot 10 v software.

3. Results

3.1. Physico-chemical characterization of AgNPs

The in-house synthesized AgNPs were analyzed through UV/VIS spectro-fluorometer and TEM analysis. UV/VIS Spectro-fluorometer revealed the presence of a characteristic SPR band of synthesized AgNPs at 450 nm (Fig. 1A). TEM analysis showed that the well-dispersed AgNPs have spherical morphology (Fig. 1B) and are within a characteristic size range of 4–12 nm. As determined using Zetasizer, the mono-dispersed size distribution of as-synthesized AgNPs shows that most of the AgNPs were of an average size of approximately 8 nm (Fig. 1C). Zeta-potential values of developed AgNPs were -3.87 ± 0.4 mV.

3.2. AgNPs affects cardiomyoblasts viability

The cytotoxic effect of AgNPs against H9c2 is shown in Fig. 2A. Exposure of H9c2 cells to AgNPs concentration of 1–10 μ g/ml demonstrated a significant inhibition of cell viability in a dose-dependent manner. After 48 hr of AgNPs treatment, cells showed significant decrease in growth to the value of 21%, as compared to control (100%) cells. The half-maximal inhibitory concentration (IC_{50}) was achieved at 3.5 μ g/ml; therefore, further experiments on H9c2 cells were performed at this concentration.

3.3. AgNPs induces DNA fragmentation

Flow cytometer analysis of DNA strand breaks is expressed as a percentage of apoptotic cells (Fig. 2B). An increase in fluorescence intensity proved that AgNPs treatment significantly induced DNA fragmentation in cells in a time-dependent manner. DNA fragmentation in AgNPs treated cells was 37% as compared to control (8%)

cells. With an increase in exposure time to 48 hr, the DNA fragmentation significantly increased to almost 40% (Fig. 2B).

3.4. AgNPs alters cell cycle phases

Flow cytometry studies were performed to further assess their effect on cell cycle distribution. As could be seen in Fig. 3, after treatment of H9c2 with AgNPs, there was a considerable accumulation of cardiomyocytes in the S phase in a time-dependent manner. As compared to control (22.77%), a significant increase of 38.12% and 48.77% in cell population was observed at 24 hr and 48 hr, respectively. An increment viz., 20.22% (24 hr) and 14.77% (48 hr) in the sub-G1 population were also seen in AgNPs treated cardiomyocytes which further implies induction of apoptotic cell death in the treatment group.

3.5. AgNPs alters cellular redox balance

The intracellular ROS levels were measured in control and AgNPs treated H9c2 cells using DCFH-DA fluorescent dye. Fig. 4 shows the results of ROS generation as examined by flow cytometry analysis and fluorescence microscopic assay. An increase in DCF fluorescence intensity proved that AgNPs treatment significantly induced ROS production in cells after 24 and 48 hr exposure. ROS generation in AgNPs treated cells was 2-fold greater than the control cells (Fig. 4A). The increase in intracellular ROS production is distinctly visualized in fluorescence images. As compared to control, the number of DCFH-DA stained ROS producing cells increased in a time-dependent manner, as screened after 24 and 48 hr (Fig. 4B).

3.6. AgNPs induces mitochondrial dysfunction

We also analyzed mitochondrial ROS levels and it was found that AgNPs treatment significantly induced mitochondrial ROS generation in H9c2 cells as evident through Mitosox analysis (Fig. 5A). As a result, to further assess that AgNPs affects mitochondrial function, ATP level in control and AgNPs treated cells were determined. It was observed that mitochondrial ATP levels were considerably reduced following treatment with AgNPs compared to control (Fig. 5B). Given that AMPK α is activated to preserve cellular energy levels, we assessed the change in AMPK1 α expression. It was found that pAMPK1 α levels were significantly enhanced to 1.5-fold after 24 hr treatment and 2.7-fold following 48 hr treatment with AgNPs (Fig. 5C).

3.7. AgNPs induces autophagy in cardiomyoblasts

Interestingly, immunofluorescence studies with important autophagy protein marker LC3BII showed that treatment with

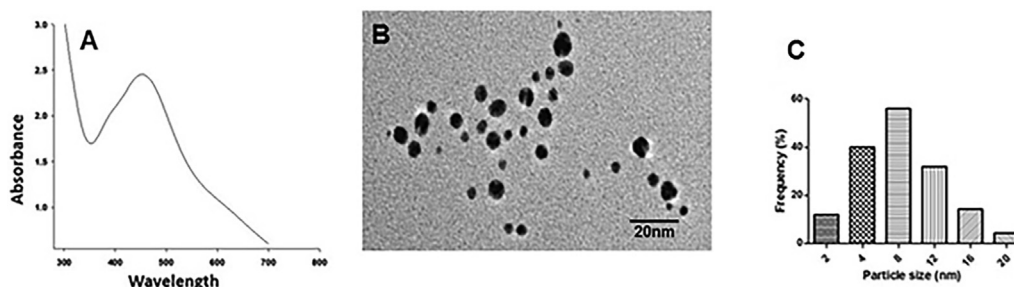


Fig. 1. Physico-chemical characteristics of the as-synthesized AgNPs were examined through UV/VIS Spectro-fluorometer. The absorption spectra were measured between 300 and 800 nm. (A) TEM image showing the size and surface morphology of the AgNPs (B) and particle size distribution analysis which is showing a characteristic size range of 4–12 nm and an average size of approximately 8 nm (C).

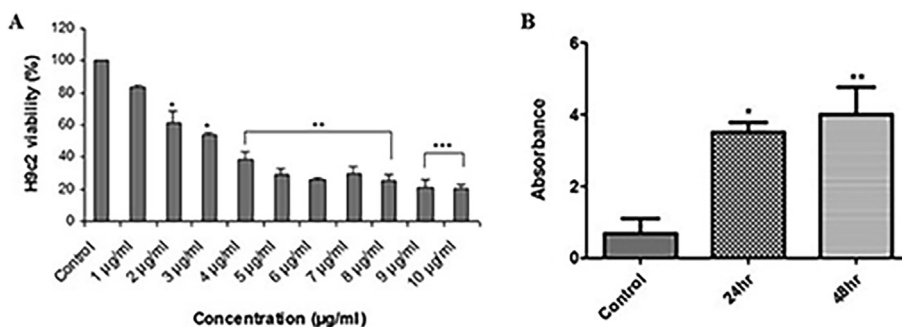


Fig. 2. AgNPs exposure affects percent viability and DNA fragmentation in H9c2 cardiac cells. (A) Cells were treated with different AgNPs concentrations from 0 to 10 µg/ml for 48 hr. Cell viability (n = 3) was evaluated by MTT reduction assay. AgNPs exposure inhibited cell viability in a dose-dependent manner. (B) BrdU analysis in control and AgNPs treated H9c2 cells following 24 hr and 48 hr time interval. Histograms show the data obtained after anti-BrdU staining. AgNPs exposure of H9c2 cells caused a significant time-dependent increase in DNA strand break signifying cell death by apoptosis. The variations in their levels were analyzed statistically. Data are presented as the mean ± SE of three independent experiments. (*p < 0.05; **p < 0.01; ***p < 0.001).

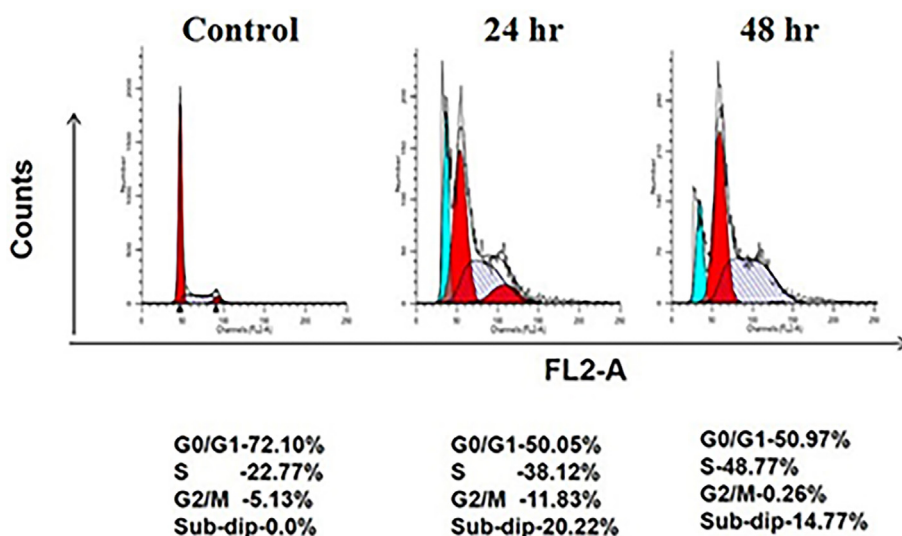


Fig. 3. AgNPs impairs cell cycle progression in H9c2 cardiac cells. Cells were treated with as-synthesized AgNPs for 24 hr and 48 hr time interval and cell percentage in each phase of the cell cycle was determined by flow cytometry. AgNPs significantly increased cell population in S-phase and interferes with G1/S transition.

AgNPs induced significant autophagy in H9c2 cells. As shown in Fig. 6, a distinct increase in LC3BII expression was visualized after 24 hr and 48 hr incubation. Further, Western blot analysis (Fig. 7) for autophagy markers, LC3BII protein expression was significantly induced in AgNPs treated cells to the level of 22% (24 hr) and 35% (48 hr). AgNPs treated cells showed a 13% increase in Beclin1 expression after 24 hr that significantly increased to 18% after 48 hr. Also, the other autophagy marker Atg5 was also observed to be significantly up-regulated following treatment with AgNPs. Atg5 expression increased significantly to 40% and 62% after 24 and 48 hr, respectively. These results instigate that AgNPs induces autophagy in H9c2 cardiac cells.

3.8. AgNPs induces cytotoxicity via the generation of ROS-ameliorates

The ameliorating effect of NAC on AgNPs induced toxicities in H9c2 cardiomyoblasts is shown in Fig. 8. RT-PCR results in Fig. 8A show a significant reduction in levels of autophagy markers in AgNPs treated cells that were pre-treated with NAC. As compared to control, levels of LC3BII were almost up-regulated to 20% in the absence of NAC. However, in the presence of NAC, AgNPs treated cells showed only 11% expression of LC3BII protein that

was comparable to the control (Fig. 8Aa). Likewise, Beclin1 levels showed a 2-fold increase in the absence of NAC (Fig. 8Ab). Here also, the presence of NAC provided protection and Beclin1 expression was insignificant. The effect of NAC was also determined on AgNPs treated cells by DNA fragmentation. BrdU assay revealed a decrease in DNA fragmentation when NAC was present (Fig. 8B). The decrease in DNA fragmentation was also distinctly visualized in agarose gel (Fig. 7C).

4. Discussion

AgNPs enjoy the status of highest commercialized nps. Since, they are widely used in industrial, biotechnological, and biomedical applications; their toxicity has become a topmost concern. Given that AgNPs can translocate through the systemic circulation and come in direct contact with the heart tissue; it is reasonable that these NPs could induce detrimental effects to the heart cells (Cameron et al., 2018). Specifically, no reports are highlighting the cytotoxic manifestations of AgNPs on cardiac cells to date. Considering this, in this research endeavor we have assessed the prospective toxicity of AgNPs on cardiac cells through cell viability, autophagy, oxidative stress, cell cycle, and apoptosis. The in-house

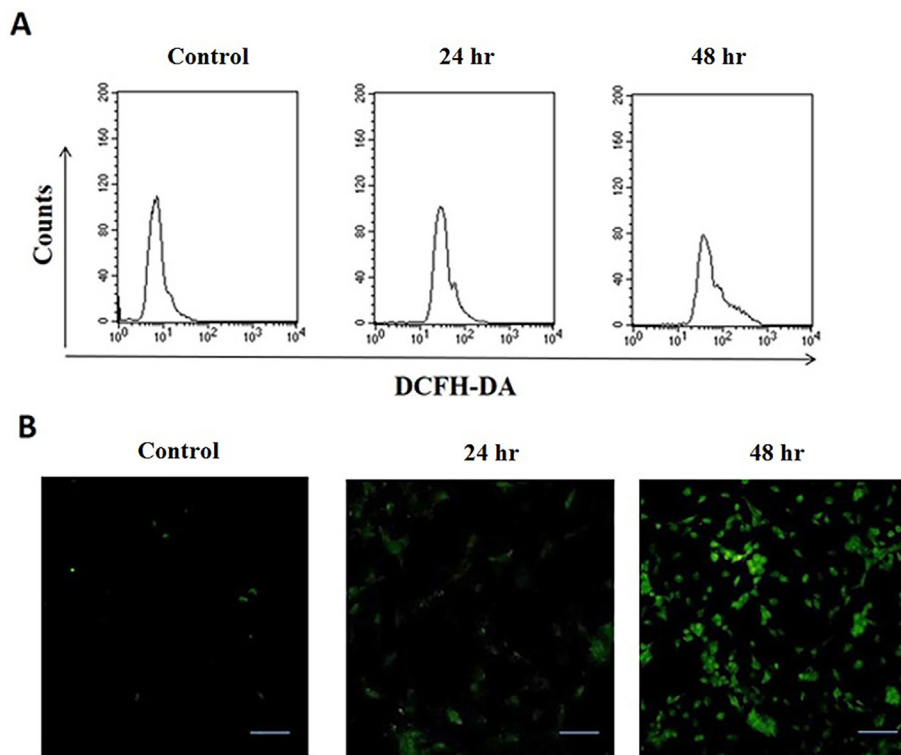


Fig. 4. ROS generation in AgNPs-treated H9c2 cardiac cells. Cells were treated with as-synthesized AgNPs for 24 hr and 48 hr time intervals and then were analyzed through DCFH-DA assay. The levels of ROS generation were detected in control and AgNPs treated H9c2 cells by (A) Flow cytometry and (B) Fluorescence microscopy.

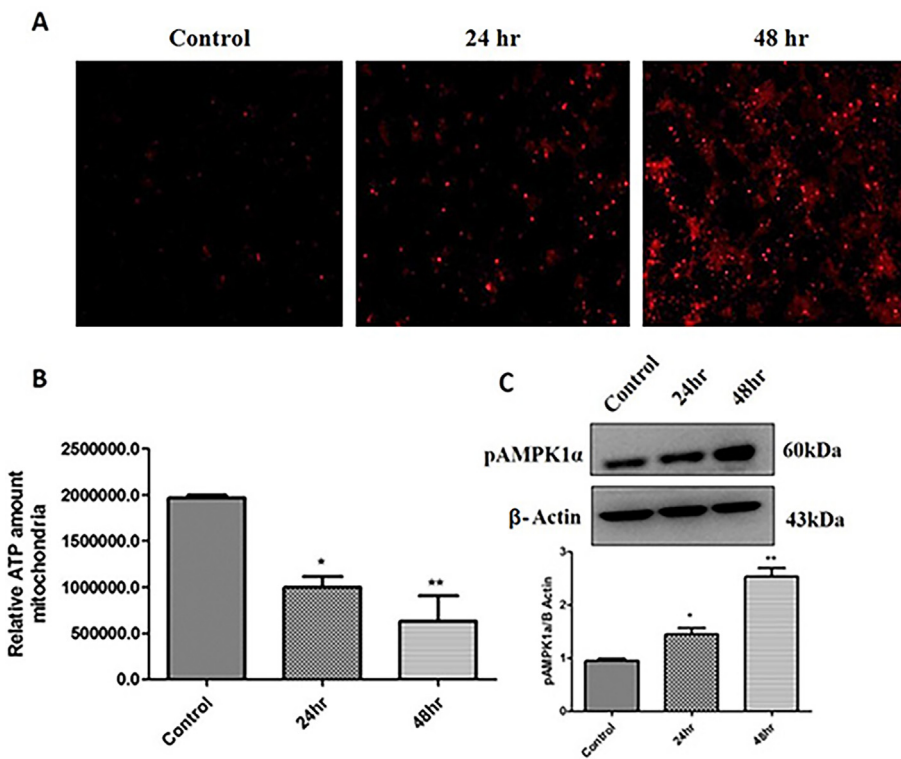


Fig. 5. AgNPs induces mitochondrial dysfunction in H9c2 cardiac cells. (A) Cells were treated with as-synthesized AgNPs for 24 hr and 48 hr time intervals and analyzed through Mitosox analysis. Representative fluorescent images were detected for confocal microscopy. Red signals represent the time-dependent increase in ROS generation in control and AgNPs treated H9c2 cells; (B) Analysis of ATP production in control and AgNPs treated H9c2 cells. The cells were treated with AgNPs for 24 hr and 48 hr and the ATP content was measured using Cell Titer-Glo Luminescent cell viability assay. The variation in ATP levels was analyzed statistically; (C) H9c2 cells were treated with AgNPs for 24 hr and 48 hr and the expression levels of pAMPK1 α marker in control and AgNPs treated cells were measured by Western blot analysis. The variations in the levels were analyzed statistically. Each column represents mean \pm SE. (* $p < 0.05$; ** $p < 0.01$).

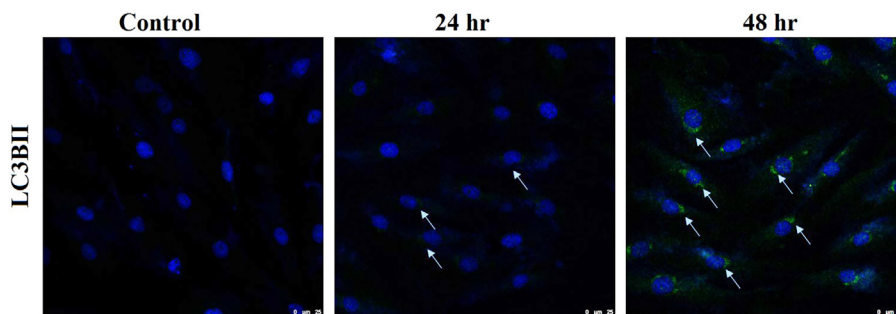


Fig. 6. Immuno stained image showing AgNPs induced autophagy in H9c2 cardiac cells. The cells were treated with as-synthesized AgNPs for 24 hr and 48 hr time intervals and were then were incubated with anti-LC3BII. Immunostaining for LC3BII autophagic marker in treated cells was visualized by fluorescence microscopy. A time-dependent increase in green signals indicates the autophagic flux in H9c2 cells.

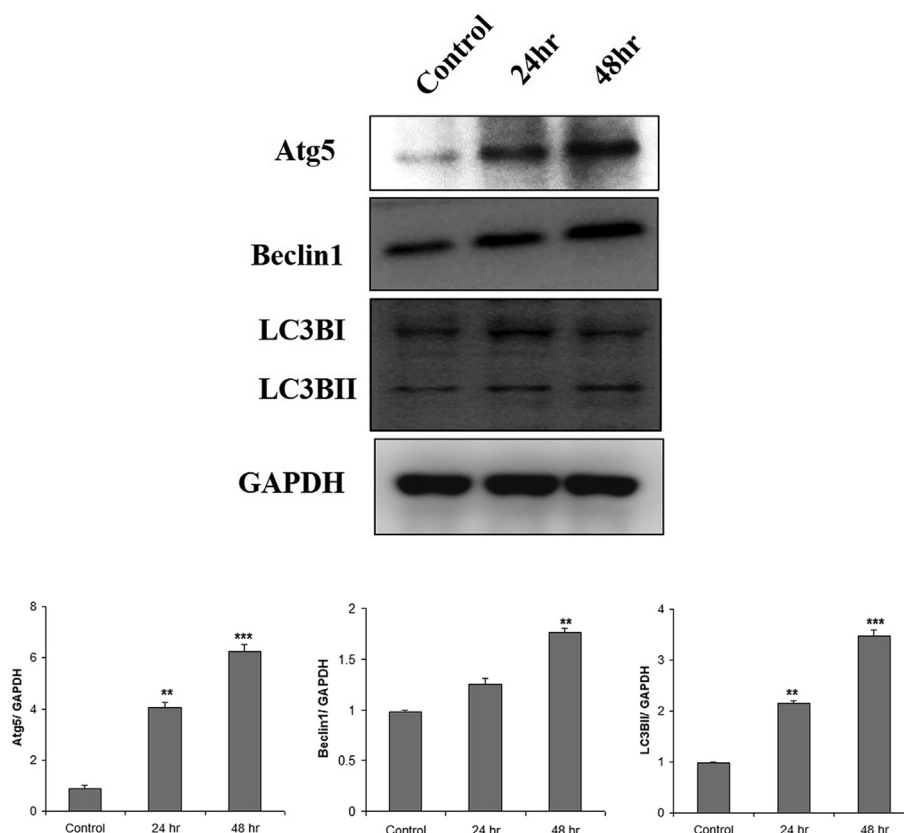


Fig. 7. AgNPs induced autophagy in H9c2 cells. Cells were treated with AgNPs for 24 hr and 48 hr and then treated with anti-autophagy proteins. Expression of LC3BII, Atg 5, Beclin1, and LC3BI in control and AgNPs treated H9c2 cells were detected by Western blot analysis. The relative protein levels were quantified by densitometry. The variations in their levels were analyzed statistically. Each column represents mean \pm SE. (* $p < 0.05$; ** $p < 0.01$; *** $p < 0.001$).

synthesized AgNPs were of ~8 nm average size and spherical in shape (Fig. 1B). They had a surface charge of -3.87 ± 0.4 mV. AgNPs induced cell toxicity was evaluated by employing a battery of tests.

Different cell types have shown variable responses upon AgNPs exposure (Nguyen et al., 2013). DNA damage, cell death or apoptosis, cell cycle arrest is some of the major effects observed on different types of cell lines after exposure to AgNPs (Akter et al., 2018). Initially, the AgNPs toxicity was evaluated by assessing the cardiomyoblasts viability (MTT assay) following exposure to different concentrations of AgNPs. Results revealed a significant decrease in cell viability in a dose-dependent manner (Fig. 2A). As far as cell cycle is concerned, AgNPs effect has been reported to be dependent on cell type, some showing arrest at S-phase and another showing at G2-phase (Akter et al., 2018; AshaRani et al., 2009; Cameron

et al., 2018). In the present study, AgNPs significantly interfered in the cell cycle of H9c2 cardiomyocytes, where an accumulation of cell population was observed in the S and sub-G1 phase (Fig. 3). The results of the treated group indicated cell death by apoptosis. Moreover, DNA fragmentation is one of the important steps in apoptosis and is used as a marker of apoptosis. Herein, AgNPs enhanced the DNA fragmentation process in a time-dependent manner (Fig. 2B).

The cellular redox system plays an imperative role in maintaining cellular homeostasis. Under normal physiological conditions, the generation of ROS and their elimination from the system is tightly regulated. However, alteration in this balance leads to various diseased states and vice-versa. Moreover, this process has been reported to be the underlying reason for cytotoxicity caused

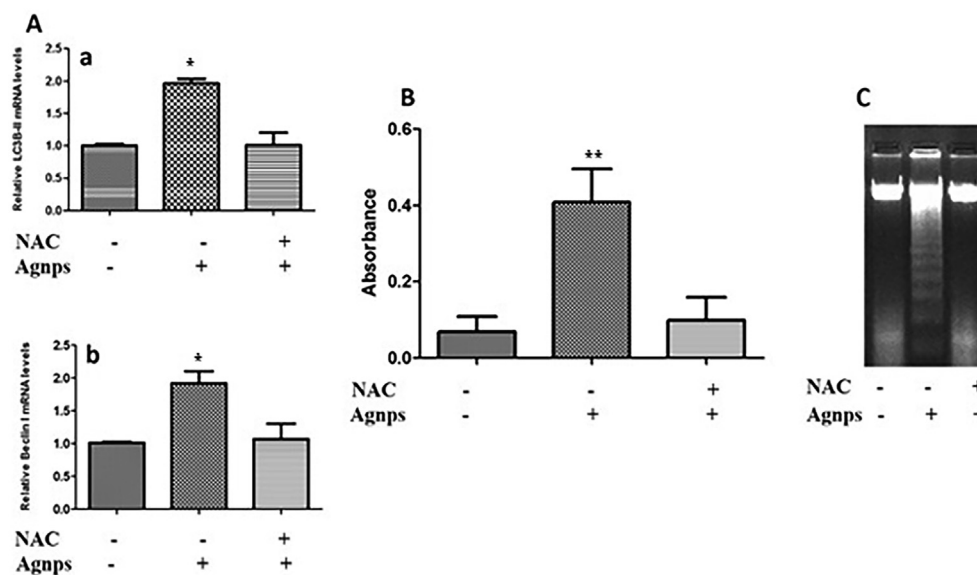


Fig. 8. Amelioration of AgNPs induced cytotoxicity in the presence of NAC. (A) Cells were pre-treated with NAC and then exposed to as-synthesized AgNPs for 48 hr. RT-PCR analysis was done to detect levels of autophagy-related markers where expression of LC3BII and Beclin1 were detected in control and AgNPs treated H9c2 cells in the absence and presence of NAC. A significant decrease in autophagy was detected in AgNPs exposed H9c2 cells pretreated with NAC; (B) BrdU analysis in control and AgNPs treated H9c2 cells in the presence and absence of NAC. Histograms show the data obtained after anti-BrdU staining. AgNPs exposure of NAC treated H9c2 cells caused a significant decrease in DNA fragmentation signifying amelioration of AgNPs toxicity; (C) DNA ladder assay in control and AgNPs treated H9c2 cells in the presence and absence of NAC. Agarose gel electrophoretic image showing the effect of AgNPs on H9c2 cells pretreated with NAC. There was a significant decrease in toxic effects of AgNPs in the presence of NAC. The variations in their levels were analyzed statistically. Each column represents mean \pm SE. (* $p < 0.05$; ** $p < 0.01$; *** $p < 0.001$).

by various NPs (Abdal Dayem et al., 2017; Das et al., 2019; Kumari et al., 2017; Verma et al., 2018). As a matter of fact, the nanosized particles due to more surface area show a higher concentration of reactive groups that result in increased cellular oxidative stress. Additionally, various signals and physiological changes lead to oxidative stress that in turn promotes apoptosis. AgNPs have been shown to produce diverse types of toxicological changes and accumulate in organs, including the heart (Gonzalez et al., 2016; Lin et al., 2017; Sambale et al., 2015). A dominant factor in the toxicity of AgNPs is the generation of ROS. Recent studies have shown AgNP-mediated ROS generation in different types of cells (AshaRani et al., 2009; Guo et al., 2015; Mohammed, 2015). A significant increase in ROS production by AgNPs exposure has been reported both in vitro and in vivo (Cho et al., 2018; Sun et al., 2016). Various cells like fibroblast, muscle and colon cells upon AgNPs exposure have shown induction of apoptosis due to increased oxidative stress (Sambale et al., 2015). In the present study also, exposure of AgNPs led to the significant production of ROS in H9c2 cells (Fig. 4).

Cell toxicity or cell damage can also be assessed by measuring mitochondrial alterations. It is widely accepted that ROS production and mitochondrial status are closely interlinked. The presence of low levels of ROS species is automatically cleared by mitochondria. However, excess ROS generation embodies the potential to induce mitochondrial damage or stress that simultaneously leads to mitochondrial dysfunction and a further increase in ROS production. Structural damage and/or mitochondria stress thereby, leads to abnormal cellular ROS balance and vice-versa (Jezek et al., 2018; Saito and Sadoshima, 2015). Since AgNPs most efficiently targets mitochondria; presently we have investigated mitochondrial ROS, AMP/ATP ratio and regulation of AMPK1 α . From the results, it is reasonable that AgNPs induces mitochondrial ROS generation, which could plausibly impact their function (Fig. 5). Actually, the induction of ROS in mitochondria might affect its functioning. After AgNPs treatment, the levels of ATP were down-regulated thereby suggesting a disturbance in mitochondrial functioning. Moreover,

alteration in AMP/ATP ratio activates AMPK1 α , which further attenuates energy-consuming processing and activates the energy-producing processes to maintain homeostasis (Hardie, 2014). Thus, given that AMPK1 α is activated to preserve cellular energy levels, we assessed the change in AMPK α expression. It was found that pAMPK α levels were considerably enhanced following treatment with AgNPs (Fig. 5). Un-regulated ROS production has been reported to ensue in autophagy owing to mitochondrial alteration (Okamoto & Kondo-Okamoto, 2012). Several cell culture studies have reported the necessity of AMPK in autophagy (Fritzen et al., 2016; Mack et al., 2012).

Autophagy is a multi-faceted phenomenon, which has aroused many clinical interests. Besides, its traditional survival-inducing function; autophagy, has been shown with putative tumor suppression function (Kroemer & Levine, 2008; Yu et al., 2013). This has led to the understanding of autophagy-mediated cell death processes. Evidence have shown that prolonged stress and excessive cellular damage plausibly lead to autophagic cell death (Mathew et al., 2007; Turcotte et al., 2008). Importantly, it has been shown that various NPs cannot be easily degraded by our cellular system; and under these circumstances, the autophagic process represents the plausible way for their elimination from the body. This is in concordance with the recent reports, wherein the authors have explicitly demonstrated the induction of autophagy by inorganic NPs (Wang et al., 2018; Zhu et al., 2017). In the present study, the expression of various protein markers of autophagy was analyzed. Treatment with AgNPs significantly induced the expression of LC3BII, Beclin 1 and Atg 5 in H9c2 cardiac cells (Figs. 6 and 7).

Accumulating evidence have highlighted the possible reduction of apoptosis upon inhibition of oxidative stress. In the current study, we assessed that whether scavenging ROS could ameliorate AgNPs induced toxicities in H9c2 cells. Interestingly, it was observed that pre-treatment with NAC, considerably reduced the autophagy markers LC3BII and Beclin1 levels in AgNPs treated cardiac cells as evident through RT-PCR analysis (Fig. 8). Besides these,

DNA fragmentation was also considerably reduced as evident through BrdU assay and agarose gel electrophoresis (Fig. 8B and C). These results, explicitly demonstrate the role of ROS in AgNPs induced cardiac toxicities (Zhu et al., 2017).

5. Conclusion

The results of the present study highlight the prospective cytotoxicity of AgNPs in H9c2 rat cardiomyoblasts. The data explicitly demonstrated that the cytotoxic response of H9c2 cells to AgNPs is time-dependent. AgNPs induces reactive oxygen species (ROS) generation, mitochondrial dysfunction mediated autophagy and cell death in cardiac cells. In view of this, the long term usage of AgNPs may create complications in the cardiac tissues severely. The study highlights that strict regulation should be enforced for the restricted usage of NPs in general and in particular AgNPs.

Declaration of Competing Interest

The authors declare that they have no known competing financial interests or personal relationships that could have appeared to influence the work reported in this paper.

Acknowledgements

The authors would like to extend their sincere appreciation to the Deanship of Scientific Research at King Saud University for funding of this research through the Research Group Project No. RGP-212.

References

- Abdal Dayem, A., Hossain, M.K., Lee, S.B., Kim, K., Saha, S.K., Yang, G.M., Choi, H.Y., Cho, S.G., 2017. The role of reactive oxygen species (ROS) in the biological activities of metallic nanoparticles. *Inter. J. Mol. Sci.* 18 (1).
- Abdeen, S., Geo, S., Sukanya, S., Praseetha, P.K., Dhanya, R.P., 2014. Biosynthesis of silver nanoparticles from *Actinomyces* for therapeutic applications. *I. J. Nano Dimen.* 5, 155–162.
- Abhilash, M., 2010. Potential applications of nanoparticles. *I. J. Pharma Bio Sci.-Bioinform.* V1 (1), 12p.
- Akter, M., Sikder, M.T., Rahman, M.M., Ullah, A., Hossain, K.F.B., Banik, S., Hosokawa, T., Saito, T., Kurasaki, M., 2018. A systematic review on silver nanoparticles-induced cytotoxicity: Physicochemical properties and perspectives. *J. Adv. Res.* 9, 1–16.
- Allison, R.R., Mota, H.C., Bagnato, V.S., Sibatia, C.H., 2008. Bionanotechnology and photodynamic therapy—state of the art review. *Photodiagnosis Photodyn. Ther.* 5 (1), 19–28.
- Anwar, M.F., Yadav, D., Rastogi, S., Arora, I., Khar, R.K., Chander, J., Samim, M., 2015. Modulation of liver and kidney toxicity by herb *Withania somnifera* for silver nanoparticles: a novel approach for harmonizing between safety and use of nanoparticles. *Protoplasma* 252, 547–558.
- AshaRani, P.V., Mun, G.L.K., Hande, M.P., Valiyaveetil, S., 2009. Cytotoxicity and genotoxicity of silver nanoparticles in human cells. *ACS Nano* 3 (2), 279–290.
- Brown, D.M., Wilson, M.R., MacNee, W., Stone, V., Donaldson, K., 2001. Size-dependent proinflammatory effects of ultrafine polystyrene particles: a role for surface area and oxidative stress in the enhanced activity of ultrafines. *Toxicol. Appl. Pharmacol.* 175, 191–199.
- Cameron, S.J., Hosseinian, F., Willmore, W.G., 2018. A current overview of the biological and cellular effects of nanosilver. *I. J. Mol. Sci.* 19, 30.
- Carmo, T.L.L., Siqueira, P.R., Azevedo, V.C., Tavares, D., Pesenti, E.C., Cestari, M.M., Martinec, C.B.R., Fernandes, M.N., 2019. Overview of the toxic effects of titanium dioxide nanoparticles in blood, liver, muscles, and brain of a Neotropical detritivorous fish. *Environ. Toxicol.* 34 (4), 457–468.
- Chernousova, S., Epple, M., 2013. Silver as antibacterial agent: Ion, nanoparticle, and metal. *Angew. Chem. Int. Ed.* 52, 1636–1653.
- Cho, Y.-M., Mizuta, Y., Akagi, J.-i., Toyoda, T., Sone, M., Ogawa, K., 2018. Size-dependent acute toxicity of silver nanoparticles in mice. *J. Toxicol. Pathol.* 31, 73–80.
- Dailey, L.A., Jekel, N., Fink, L., Gessler, T., Schmehl, T., Wittmar, M., Kissel, T., Seeger, W., 2006. Investigation of the proinflammatory potential of biodegradable nanoparticle drug delivery systems in the lung. *Toxicol. Appl. Pharmacol.* 215, 100–108.
- Das, B.K., Verma, S.K., Das, T., Panda, P.K., Parashar, K., Suar, M., Parashar, S.K.S., 2019. Altered electrical properties with controlled copper doping in ZnO nanoparticles infers their cytotoxicity in macrophages by ROS induction and apoptosis. *Chemico-Biol. Interac.* 297, 141–154.
- Edmundson, M.C., Capeness, M., Horsfal, L., 2014. Exploring the potential of metallic nanoparticles within synthetic biology. *New Biotechnol.* 31 (6), 572–578.
- Emeje, M.O., Obidike, I.C., Akpabio, E.I., Ofoefule, S.I., 2012. Nanotechnology in Drug Delivery. Chapter 4 in *Recent Advances in Novel Drug Carrier Systems*, In Tech Publisher doi:10.5772/51384.
- Emerich, D.F., Thanos, C.G., 2003. Nanotechnology and medicine. *Expert Opin. Biol. Ther.* 3 (4), 655–663.
- Fageria, L., Pareek, V., Dilip, R.V., Bhargava, A., Pasha, S.S., Laskar, I.R., Saini, H., Dash, S., Chowdhury, R., Panwar, J., 2017. Biosynthesized protein-capped silver nanoparticles induce ROS-dependent proapoptotic signals and pro-survival autophagy in cancer cells. *ACS Omega* 2, 1489–1504.
- Fritzen, A.M., Frøsig, C., Jeppesen, J., Jensen, T.E., Lundsgaard, A.-M., Serup, A.K., Schjærling, P., Proud, C.G., Richter, E.A., Kiens, B., 2016. Role of AMPK in regulation of LC3 lipidation as a marker of autophagy in skeletal muscle. *Cell. Signal.* 28, 663–674.
- Gonzalez, C., Rosas-Hernandez, H., Ramirez-Lee, M.A., Salazar-Garcia, S., Ali, S.F., 2016. Role of silver nanoparticles (AgNPs) on the cardiovascular system. *Arch. Toxicol.* 90, 493–511.
- Guo, H., Zhang, J., Boudreau, M., Meng, J., Yin, J.-j., Liu, J., Xu, H., 2015. Intravenous administration of silver nanoparticles causes organ toxicity through intracellular ROS-related loss of inter-endothelial junction. *Part. Fibre Toxicol.* 13 (1), 21.
- Gurunathan, S., Han, J.W., Park, J.H., Kim, E., Choi, Y.J., Kwon, D.N., Kim, J.H., 2015. Reduced graphene oxide-silver nanoparticle nanocomposite: A potential anticancer nanotherapy. *I. J. Nanomed.* 10, 6257–6276.
- Hamoir, J., Nemmar, A., Halloy, D., Wirth, D., Vincke, G., Vanderplasschen, A., Nemery, B., Gustin, P., 2003. Effect of polystyrene particles on lung microvascular permeability in isolated perfused rabbit lungs: role of size and surface properties. *Toxicol. Appl. Pharmacol.* 190, 278–285.
- Hardie, D.G., 2014. AMPK-sensing energy while talking to other signaling pathways. *Cell Metabol.* 20 (6), 939–952.
- Holland, N.A., Thompson, L.C., Vidanapathirana, A.K., Urankar, R.N., Lust, R.M., Fennell, T.R., Wingard, C.J., 2016. Impact of pulmonary exposure to gold core silver nanoparticles of different size and capping agents on cardiovascular injury. *Part. Fibre Toxicol.* 13, 48.
- Holmila Reetta, J., Vance, S.A., King, S.B., Tsang, A.W., Singh, R., Furdul, C.M., 2019. Silver nanoparticles induce mitochondrial protein oxidation in lung cells impacting cell cycle and proliferation. *Antioxidants* 8, 552–567.
- Hu, C.-M.J., Aryal, S., Zhang, L., 2010. Nanoparticle-assisted combination therapies for effective cancer treatment. *Ther. Del.* 1 (2), 323–334.
- Huerta-Garcia, E., Zepeda-Quiroz, I., Sanchez-Barrera, H., Colin-Val, Z., Alfaro-Moreno, E., Ramos-Godinez, M.D.P., Lopez-Marure, R., 2018. Internalization of titanium dioxide nanoparticles is cytotoxic for H9c2 rat cardiomyoblasts. *Molecules* 23 (8). <https://doi.org/10.3390/molecules23081955>.
- Hussain, J.I., Kumar, S., Hashmi, A.A., Khan, Z., 2011. Silver nanoparticles: preparation, characterization, and kinetics. *Adv. Mater. Lett.* 2, 188–194.
- Iovine, B., Iannella, M.L., Nocella, F., Pricolo, M.R., Bevilacqua, M.A., 2012. Carnosine inhibits KRAS-mediated HCT116 proliferation by affecting ATP and ROS production. *Cancer Lett.* 315 (2), 122–128.
- Iravani, S., Korbekandi, H., Mirmohammadi, S.V., Zolfaghari, B., 2014. Synthesis of silver nanoparticles: chemical, physical and biological methods. *Res. Pharma. Sci.* 9 (6), 385–406.
- Jezek, J., Cooper, K.F., Strich, R., 2018. Reactive oxygen species and mitochondrial dynamics: the yin and yang of mitochondrial dysfunction and cancer progression. *Antioxidants* 7, 13.
- Jiang, Z.F., Shao, L.J., Wang, W.M., Yan, X.B., Liu, R.Y., 2012. Decreased expression of Beclin-1 and LC3 in human lung cancer. *Molec. Biol. Rep.* 39 (1), 259–267.
- Joviano-Santos, J.V., Sa, M.A., Maria, M.L., Almeida, T.C., Geraldo, V., Oliveira, S., Ladeira, L.A., Ferreira, A.J., 2014. Evaluation of cardiovascular toxicity of carbon nanotubes functionalized with sodium hyaluronate in oral regenerative medicine. *Braz. J. Med. Biol. Res.* 47 (7), 560–566.
- Karthik, L., Kumar, G., Vishnu-Kirthi, A., Rahuman, A.A., Rao, V.B., 2014. *Streptomyces* sp. LK3 mediated synthesis of silver nanoparticles and its biomedical application. *Bioprocess Biosys. Eng.* 37, 261–267.
- Kavosi, A., Hosseini, Ghale, Noei, S., Madani, S., Khalighfar, S., Khodayari, S., Khodayari, H., Mirzaei, M., Kalhori, M.R., Yavarian, M., Alizadeh, A.M., Falahati, M., 2018. The toxicity and therapeutic effects of single- and multi-wall carbon nanotubes on mice breast cancer. *Sci. Rep.* 8 (1), 8375.
- Khan, A.A., Alam, M., Tufail, S., Mustafa, J., Owais, M., 2011. Synthesis and characterization of novel PUFA esters exhibiting potential anticancer activities: An *in vitro* study. *Eur. J. Med. Chem.* 46, 4878–4886.
- Khan, A.A., 2017. Pro-apoptotic activity of nano-escheriosome based oleic acid conjugate against 7, 12-dimethylbenz (a) anthracene (DMBA) induced cutaneous carcinogenesis. *Biomed. Pharmacother.* 90, 295–302.
- Khan, B.F., Hamidullah, K., Dwivedi, S., Konwar, R., Zubair, S., Owais, M., 2018. Potential of bacterial culture media in biofabrication of metal nanoparticles and the therapeutic potential of the as-synthesized nanoparticles in conjunction with artemisinin against MDA-MB-231 breast cancer cells. *J. Cell. Physiol.* 234, 6951–6964.
- Khan, A.A., Alanazi, A.M., Jabeen, M., Chauhan, A., Ansari, M.A., 2019. Therapeutic potential of functionalized siRNA nanoparticles on regression of liver cancer in experimental mice. *Sci. Rep.* 9 (1), 15825–15840.
- Kroemer, G., Levine, B., 2008. Autophagic cell death: the story of a misnomer. *Nature Rev. Mol. Cell Biol.* 9 (12), 1004–1010.

- Kumar, V., Wadhwa, R., Kumar, N., Maurya, P.K., 2019. A comparative study of chemically synthesized and *Camellia sinensis* leaf extract-mediated silver nanoparticles. *3. Biotechnol.* 9 (1), 7.
- Kumari, P., Panda, P.K., Jha, E., Kumari, K., Nisha, K., Mallick, M.A., Verma, S.K., 2017. Mechanistic insight to ROS and Apoptosis regulated cytotoxicity inferred by Green synthesized CuO nanoparticles from *Calotropis gigantea* to Embryonic Zebrafish. *Sci. Rep.* 7 (1), 16284.
- Ladhar, C., Geffroy, B., Cambier, S., Treguer-Delapierre, M., Durand, E., Brethes, D., Bourdineaud, J.P., 2014. Impact of dietary cadmium sulphide nanoparticles on Danio rerio zebrafish at very low contamination pressure. *Nanotoxicol.* 8 (6), 676–685.
- Lee, Y.H., Cheng, F.Y., Chiu, H.W., Tsai, J.C., Fang, C.Y., Chen, C.W., Wang, Y.J., 2014. Cytotoxicity, oxidative stress, apoptosis and the autophagic effects of silver nanoparticles in mouse embryonic fibroblasts. *Biomater.* 35, 4706–4715.
- Li, C.Y., Zhang, Y.J., Oei, J.D., Zhao, W.W., Chu, L., DeSilva, M.N., Ghimire, A., Rawls, H. R., et al., 2012. Antimicrobial acrylic materials with in situ generated silver nanoparticles. *J. Biomed. Mat. Res. B Appl. Biomater.* 100 (2), 409–415.
- Lin, C.X., Yang, S.Y., Gu, J.L., Meng, J., Xu, H.Y., Cao, J.M., 2017. The acute toxic effects of silver nanoparticles on myocardial transmembrane potential, INa and IK1 channels and heart rhythm in mice. *Nanotoxicol.* 11, 827–837.
- Mack, H.I., Zheng, B., Asara, J.M., Thomas, S.M., 2012. AMPK-dependent phosphorylation of ULK1 regulates ATG9 localization. *Autophagy* 8 (8), 1197–1214.
- Mohammed, A.E., 2015. Green synthesis, antimicrobial and cytotoxic effects of silver nanoparticles mediated by *Eucalyptus camaldulensis* leaf extract. *Asian Pacific J. Trop. Biomed.* 5 (5), 382–386.
- Mathew, R., Karantza-Wadsworth, V., White, E., 2007. Role of autophagy in cancer. *Nat. Rev. Cancer.* 7 (12), 961–967.
- Mukhopadhyay, P., Rajesh, M., Yoshihiro, K., Hasko, G., Pacher, P., 2007. Simple quantitative detection of mitochondrial superoxide production in live cells. *Biochem. Biophys. Res. Commun.* 358 (1), 203–208.
- Nemmar, A., Vanbilloen, H., Hoylaerts, M.F., Hoet, P.H., Verbruggen, A., Nemery, B., 2001. Passage of intratracheally instilled ultrafine particles from the lung into the systemic circulation in hamster. *Amer. J. Respir. Crit. Care Med.* 164 (9), 1665–1668.
- Nikalje, A.P., 2015. Nanotechnology and its applications in medicine. *Med. Chem.* 5 (2), 081–089.
- Nguyen, K.C., Seligy, V.L., Massarsky, A., Moon, T.W., Rippstein, P., Tan, J., Tayabali, A. F., 2013. Comparison of toxicity of uncoated and coated silver nanoparticles. *J. Phys. Conf. Ser.* 429, 012025.
- Oberdorster, G., 2001. Pulmonary effects of inhaled ultrafine particles. *Inter. Arch. Occupat. Environ. Health* 74 (1), 1–8.
- Okamoto, K., Kondo-Okamoto, N., 2012. Mitochondria and autophagy: critical interplay between the two homeostats. *Biochim. Biophys. Acta.* 1820 (5), 595–600.
- Pujalte, I., Passagne, I., Brouillaud, B., Treguer, M., Durand, E., Ohayon-Courtes, C., L'Azou, B., 2011. Cytotoxicity and oxidative stress induced by different metallic nanoparticles on human kidney cells. *Part. Fibre Toxicol.* 8, 10.
- Quadros, M.E., Marr, L.C., 2010. Environmental and human health risks of aerosolized silver nanoparticles. *J. Air Waste Management Assoc.* 60 (7), 770–781.
- Rahman, M.F., Wang, J., Patterson, T.A., Saini, U.T., Robinson, B.L., Newport, G.D., Murdock, R.C., Schlager, J.J., Hussain, S.M., Ali, S.F., 2009. Expression of genes related to oxidative stress in the mouse brain after exposure to silver-25 nanoparticles. *Toxicol. Lett.* 187 (1), 15–21.
- Rana, K., Verma, Y., Rani, V., Rana, S.V.S., 2018. Renal toxicity of nanoparticles of cadmium sulphide in rat. *Chemosphere* 193, 142–150.
- Ratan, Z.A., Haidere, M.F., Nurunnabi, M., Shahriar, S.M., Ahammad, A.J.S., Shim, Y.Y., Reaney, M.J.T., Cho, J.Y., 2020. Green chemistry synthesis of silver nanoparticles and their potential anticancer effects. *Cancers (Basel)* 12 (4), 855.
- Saito, T., Sadoshima, J., 2015. Molecular mechanisms of mitochondrial autophagy/mitophagy in the heart. *Circ. Res.* 116, 1477–1490.
- Sambale, F., Wagner, S., Stahl, F., Khaydarov, R.R., Scheper, T., Bahnmann, D., 2015. Investigations of the toxic effect of silver nanoparticles on mammalian cell lines. *J. Nanomat.* Article ID 136765, 9 pages.
- Service, R.F., 2004. Nanotoxicology. *Nanotechnology grows up. Science* 304 (5678), 1732–1734.
- Shankar, S., Rhim, J.W., 2015. Amino acid mediated synthesis of silver nanoparticles and preparation of antimicrobial agar/silver nanoparticles composite films. *Carbohydr. Polym.* 130, 353–363.
- Sintubin, L., De, G.B., Van der, M.P., Pycke, B.F., Verstraete, W., Boon, N., 2011. The antibacterial activity of biogenic silver and its mode of action. *Appl. Microbiol. Biotechnol.* 91, 153–162.
- Srinivasan, M., Rajabi, M., Mousa, S.A., 2015. Multifunctional nanomaterials and their applications in drug delivery and cancer therapy. *Rev. Nanomat.* 5, 1690–1703.
- Sun, C., Yin, N., Wen, R., Liu, W., Jia, Y., Hu, L., Zhou, Q., Jiang, G., 2016. Silver nanoparticles induced neurotoxicity through oxidative stress in rat cerebral astrocytes is distinct from the effects of silver ions. *Neurotoxicol.* 52, 210–221.
- Sun, T., Seff, K., 2011. Silver clusters and chemistry in zeolites. *Chem. Rev.* 94, 857–870.
- Sunkar, S., Nachiyar, C.V., 2012. Biogenesis of antibacterial silver nanoparticles using the endophytic bacterium *Bacillus cereus* isolated from *Garcinia xanthochymu*. *Asian Pacific J. Trop. Biomed.* 12, 953–959.
- Turcotte, S., Chan, D.A., Sutphin, P.D., Hay, M.P., Denny, W.A., Giaccia, A.J., 2008. A molecule targeting VHL-deficient renal cell carcinoma that induces autophagy. *Cancer Cell* 14 (1), 90–102.
- Verma, S.K., Jha, E., Panda, P.K., Mukherjee, M., Thirumurugan, A., Makkar, H., Das, B., Parashar, S.K.S., Suar, M., 2018. Mechanistic insight into ROS and neutral lipid alteration induced toxicity in the human model with fins (*Danio rerio*) by industrially synthesized titanium dioxide nanoparticles. *Toxicol. Res.* 7 (2), 244–257.
- Wang, E.C., Wang, A.Z., 2014. Nanoparticles and their applications in cell and molecular biology. *Integ. Biol.* 6 (1), 9–26.
- Wang, Q., Zhou, Y., Fu, R., Zhu, Y., Song, B., Zhong, Y., Wu, S., Shi, Y., Wu, Y., Su, Y., Zhang, H., He, Y., 2018. Distinct autophagy-inducing abilities of similar-sized nanoparticles in cell culture and live *C. elegans*. *Nanoscale.* 10 (48), 23059–23069.
- Watkins, S.J., Borthwick, G.M., Arthure, H.M., 2011. The H9C2 cell line and primary neonatal cardiomyocyte cells show similar hypertrophic responses in vitro. *Vitro Cell. Dev. Biol. Anim.* 47, 125–131.
- Xu, Q.H., Guan, P., Zhang, T., Lu, C., Li, G., Liu, J.X., 2018. Silver nanoparticles impair zebrafish skeletal and cardiac myofibrillogenesis and sarcomere formation. *Aquat. Toxicol.* 200, 102–113.
- Yu, K.N., Yoon, T.J., Minai-Tehrani, A., Kim, J.E., Park, S.J., Jeong, M.S., Ha, S.W., Lee, J. K., Kim, J.S., Cho, M.H., 2013. Zinc oxide nanoparticle induced autophagic cell death and mitochondrial damage via reactive oxygen species generation. *Toxicol. In Vitro.* 27 (4), 1187–1195.
- Zhang, S., Tang, Y., Vlahovic, B., 2016. A review on preparation and applications of silver-containing nanofibers. *Nanoscale Res. Lett.* 11 (1), 80.
- Zhu, L., Guo, D., Sun, L., Huang, Z., Zhang, X., Ma, W., Wu, J., Xiao, L., Zhao, Y., Gu, N., 2017. Activation of autophagy by elevated reactive oxygen species rather than released silver ions promotes cytotoxicity of polyvinylpyrrolidone-coated silver nanoparticles in hematopoietic cells. *Nanoscale* 9 (17), 5489–5498.